A Pictorial Review of Pelvic Pain—Beyond the Genitourinary System

Crysta Iv Kyrazis, MD and Dhanashree Rajderkar, MD†*

Abstract: Pelvic pain may be caused by disorders of the reproductive, urinary, or gastrointestinal systems. In the pediatric population, pelvic pain is often first evaluated with ultrasonography, with other imaging modalities reserved for further workup or specific indications. Radiologists must be aware of the findings associated with common pelvic emergencies to allow prompt diagnosis and prevention of life-threatening complications. Although the range of pelvic pathology is extensive, this pictorial review presents ultrasound examples of common nontraumatic causes of pelvic pain encountered in the pediatric population, with a brief discussion about multimodality imaging features.

Key Words: multimodality imaging, nontraumatic, pediatric population, pelvic emergencies, pelvic pain, ultrasound.

(*Ultrasound Quarterly* 2022;00: 00–00)

Pelvic pain can result from disorders of the reproductive, urinary, or gastrointestinal (GI) systems. Diagnosing the etiology of pain can be difficult, and clinical and laboratory evaluation is often not sufficient. In pediatric patients, ultrasound (US) is the imaging modality of choice in the initial evaluation of pelvic pain, because it does not utilize ionizing radiation and is relatively quick and easy to perform. Plain radiographs are rarely useful for diagnosing the cause of pelvic pain. More advanced modalities such as computed tomography (CT) and magnetic resonance imaging (MRI) are reserved for further workup or specific indications. In pelvic emergencies, recognizing typical imaging findings is important for timely diagnosis and prevention of morbid or life-threatening complications, such as loss of ovarian function, appendiceal rupture, hemoperitoneum, or even death.

The purpose of this article is to provide examples of characteristic US imaging features of common nontraumatic causes of pediatric pelvic pain and to provide a few complementary examples using other modalities.

Received for publication February 4, 2021; accepted March 16, 2022.

*Department of Radiology, University of Michigan, Ann Arbor, MI; and †Department of Radiology, Division of Pediatric Radiology, University of Florida, Gainesville, FL.

The authors declare no conflict of interest.

Address correspondence to: Dhanashree Rajderkar, MD, Division of Pediatric Radiology, Department of Radiology, University of Florida College of Medicine, PO Box 100374, Gainesville, FL 32610 (e-mail: rajdda@radiology.ufl.edu).

DOI: 10.1097/RUQ.0000000000000625

US Technique

Using the distended bladder as an acoustic window, high-resolution pelvic US allows detailed evaluation of the lower urinary tract, uterus and adnexa, prostate and seminal vesicles, and pelvic vasculature. This is performed in transverse and sagittal planes using phased array or curvilinear transducers, ranging from 3 to 12 MHz, depending on the size of the patient and organ of interest.[1]

In adults, transabdominal (TAS) and transvaginal (TVS) sonography for the female pelvis are complementary procedures. Transabdominal sonography is a less invasive procedure that provides a more global field of view, but it can be limited by body habitus, anatomy (eg, retroverted uterus), artifact from bowel gas, or incomplete distention of the urinary bladder. Using higher-frequency transducers and an endovaginal approach, TVS provides better image resolution and thus better characterization of adnexal and endometrial abnormalities within a smaller field of view. However, performing an endovaginal examination in a pediatric patient is potentially traumatic, and TVS should be limited to consenting adolescent patients who have previously had a speculum examination or who have been sexually active.

GYNECOLOGIC ETIOLOGIES

Brief Summary of Pediatric Gynecologic Anatomy

At birth, because of the influence of maternal and placental hormones in utero, the neonatal uterus and ovaries are comparatively large in size; the cervix is initially disproportionately bulbous; and the endometrium is echogenic and well visualized, often with trace endometrial fluid. After the first 3 to 4 months, hormone levels and their effects on the infant reproductive tract decrease. Throughout infancy and early childhood, the uterus is approximately 3 cm longitudinally and 1 cm anteroposterior or transverse; the cervix is similar in thickness to the uterine fundus; the endometrium may be visible as a thin echogenic line; and the ovaries are approximately 1 cm^3 in volume.[2] As a female develops, these organs remain relatively unchanged until the first growth spurt at approximately 7 to 8 years old, whereupon they gradually increase in size until puberty. After puberty, the uterine fundus becomes thicker and elongates compared with the cervix; the endometrium becomes more visible on US as it begins to cycle for menstruation; and the ovaries average 6 to 10 cm^3 in volume. Mature ovarian follicles may be present at any point of development because of pervasive secretion of follicle-stimulating hormone, although they are less common from 1 to 7 years old.[3]

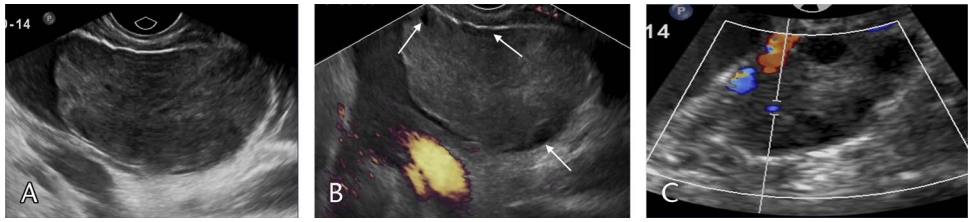

FIGURE 1. Ovarian torsion in a 16-year-old female patient. A, Gray-scale TVS in the transverse plane demonstrates an enlarged ovary with echogenic stroma. B, Transverse US with power Doppler shows complete lack of vascularity with peripheralization of small fluid-filled follicles (white arrows). C, Note the normal contralateral ovary with preserved arterial and venous flow on transverse US with color Doppler.

Adnexal Torsion

Ovarian torsion results from partial or complete twisting of the ovary about its pedicle, causing occlusion of the ovarian artery, vein, and lymphatic drainage. This can lead to ovarian necrosis unless corrected early. Prompt diagnosis is critical, as ovarian function sharply declines after 48 hours from onset of symptoms.[4]

In pediatrics, ovarian torsion occurs in a bimodal age distribution, with 16% occurring in infants (<1 year old) and 52% occurring in the peripubertal age group (9–14 years old).[5] Torsion can occur in a normal ovary in children because of adnexal hypermobility from elongated fallopian tubes and laxity of supporting ligaments. Similar to adults, an ovarian cyst or mass further increases the risk of torsion due to adnexal enlargement, which acts as a lead point for twisting about the ovarian pedicle. Mature cystic teratomas are the most common type of ovarian mass in children and are associated with torsion in up to 30% of cases.[6]

The most common sonographic finding of ovarian torsion is an enlarged heterogeneous ovary, with a median volume 12 times that of the normal contralateral ovary.[7] Other sonographic findings include enlarged peripheral follicles and detection of a lead point or mass, with the presence of a 5-cm or larger adnexal mass highly suggestive of torsion.[5] Visualization of a twisted vascular pedicle is pathognomonic, which can appear as swirling of the vasculature in cross section ("whirlpool sign") or a thickened beaklike tubular appearance longitudinally. Hypervascularization of follicles or complete absence of adnexal flow may be seen on Doppler. However, arterial flow can be present in 40% of torsed ovaries because of the ovary's dual arterial supply from the aorta via the ovarian artery and from the ovarian branch of the uterine artery.[8] On CT and MRI, similar imaging findings are typical with heterogeneous ovarian enlargement, variable degrees of contrast enhancement, and less commonly twisting of the vascular pedicle; secondary edematous or ischemic changes may be seen (Figs. 1–3).

Hemorrhagic Ovarian Cyst

Hemorrhagic ovarian cysts occur when corpus luteal or follicular ovarian cysts develop internal hemorrhage. Corpus luteal cysts are more commonly involved particularly after ovulation because of increased vascularity during the luteal phase. A hemorrhagic ovarian cyst typically manifests as a self-limited event with abrupt-onset severe pelvic pain midmenstrual cycle. In severe cases, however, active hemorrhage after rupture can lead to life-threatening hemoperitoneum and hypovolemic shock.

Sonographic features differ, depending on time course and amount of hemorrhage. Ultrasound findings may not be specific; however, 90% of hemorrhagic cysts demonstrate a lacelike reticular pattern or retracting clot.[9] In the hyperacute phase, a nonspecific hyperechoic ovarian mass with posterior through-transmission may be seen. Fibrin strands from blood products begin to organize within the first 24 hours, and a diagnostic lacelike reticular pattern with low-level internal echoes can be seen in the acute and subacute phases. Other findings include fluid-fluid levels, persistent posterior acoustic enhancement, and lack of internal vascularity. Ruptured hemorrhagic cyst can be suggested with the presence of a retracted ovarian cyst and complex free fluid suggesting hemoperitoneum. On follow-up US, as the clot retracts over the next weeks, it becomes gradually more hyperechoic and smaller in size with sharp retracting borders ("retracting clot sign"). Computed

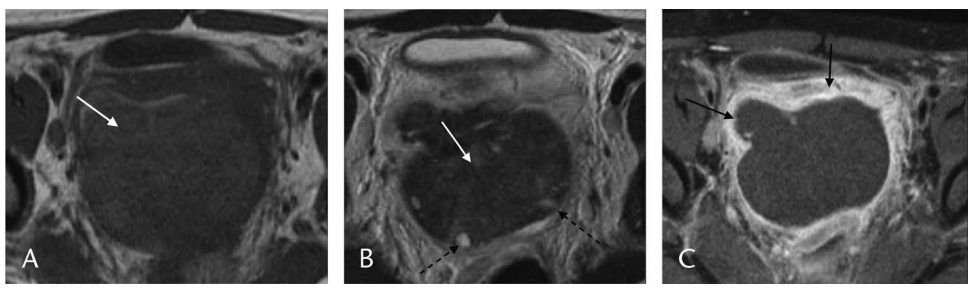

FIGURE 2. Right ovarian infarct with peripheral hyperperfusion in an 8-year-old girl. Axial T1-weighted (A), T2-weighted (B), and postcontrast T1-weighted (C) MRI images show an enlarged right ovary (white arrows) with tiny peripheral follicles (black dotted arrows) and increased vascularity at the periphery (black arrows) of the right ovary.

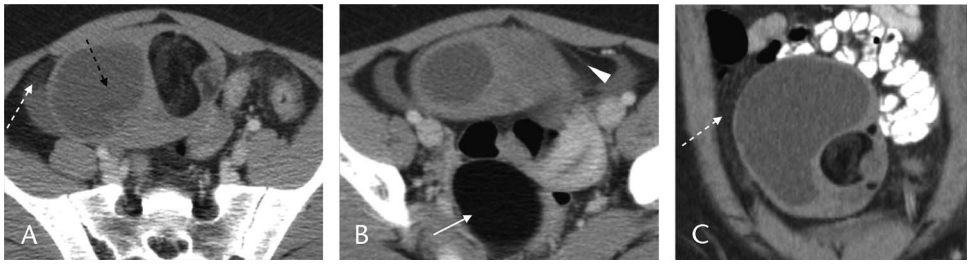

FIGURE 3. Bilateral ovarian teratomas with left ovarian torsion in a 13-year-old female patient presenting with severe pelvic pain. Axial (A, B) and coronal (C) contrast-enhanced CT images demonstrate a torsed left ovarian teratoma (black dotted arrow), which lies in the right hemipelvis with adjacent fat stranding (white dotted arrows), free fluid, and increased vascular congestion (white arrowhead). An uncomplicated right ovarian teratoma (white arrow) is seen in the pelvis posteriorly.

tomography may show hyperattenuation (>40 Hounsfield units) or fluid-fluid levels within an ovarian cyst, and hemoperitoneum is possible in cases of rupture[10] (Figs. 4 and 5).

Ectopic Pregnancy

Ectopic pregnancy occurs when a blastocyst implants outside the endometrial canal. Nearly 95% of ectopic pregnancies occur in the fallopian tubes, particularly the ampulla. Interstitial, cornual, cervical, ovarian, cesarean scar, intra-abdominal, and heterotopic ectopic pregnancies are less common.[11] Adolescents have the lowest incidence of ectopic pregnancy but the highest mortality rate.[12]

Diagnosis is typically with TAS or TVS correlated with serum β-human chorionic gonadotropin (β-hCG) levels. While diagnostic serum β-hCG levels may vary by institution, an intrauterine pregnancy should be visible by TVS with a β-hCG of 2000 mIU/mL and by TAS with a β-hCG of 6500 mIU/mL.[13,14] In patients with threshold β-hCG levels, the absence of an intrauterine pregnancy should raise concern for possible ectopic implantation. The most common sonographic finding is a cystic adnexal mass distinct from the ipsilateral ovary, representing a gestational sac or yolk sac with embryo. An extraovarian echogenic tubal ring may also be identified with peripheral hypervascularity ("tubal ring" or "ring of fire sign"). Computed tomography findings include a cystic adnexal mass with peripheral enhancement or surrounding hemoperitoneum in cases of rupture (Fig. 6).

Pelvic Inflammatory Disease

Pelvic inflammatory disease (PID) occurs most commonly because of ascending infection from vaginal flora or sexually transmitted microorganisms. This results in inflammation of the upper reproductive tract, including endometritis or salpingitis.

Ultrasound findings of endometritis include heterogeneous endometrial thickening with an indistinct endometrial-echo complex and an enlarged, hyperechoic uterus. In salpingitis, the nondilated fallopian tubes become inflamed, with subtle US findings of tubal wall thickening and mural hypervascularity. Prominent bilateral adnexa adherent to the uterus is indicative of salpingo-oophoritis and can be seen in the acute phase of PID ("koala sign" given the resemblance to a koala's face).[15]

Salpingitis can cause adhesions that lead to distal tubal obstruction, preventing drainage of fluid. This may result in hydrosalpinx or pyosalpinx, in which an infected fallopian tube becomes distended with serous or purulent fluid, respectively. On US, hydrosalpinx appears as a dilated, thin-walled, serpiginous fallopian tube with simple fluid. Pyosalpinx may appear similar on US but is more likely to have bilateral involvement with thickened walls, echogenic fluid and debris, and mural hyperemia. Computed tomography demonstrates fallopian tubes

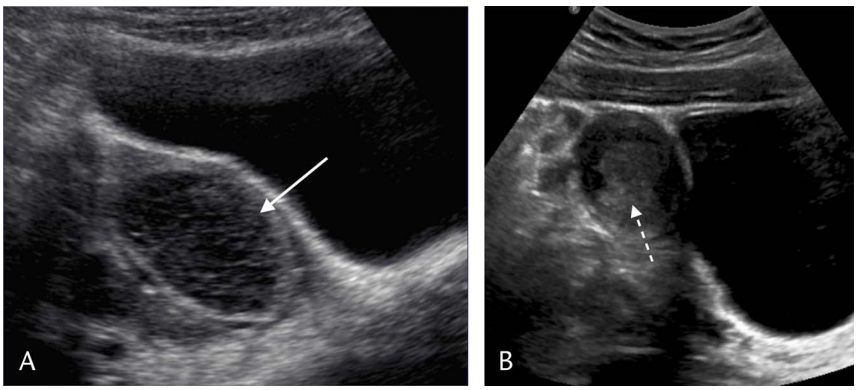

FIGURE 4. Hemorrhagic ovarian cyst, classic signs in 2 different patients. A, A 16-year-old female patient: transabdominal sagittal US of the adnexa shows a complex ovarian cyst with a characteristic echogenic, lacelike reticular pattern (white arrow), representing fibrin strands within a hemorrhagic cyst. B, A 12-year-old female patient: transabdominal sagittal US shows the sharp, concave borders of an echogenic clot (white dotted arrow) within a right ovarian cyst, representing the retracting clot sign.

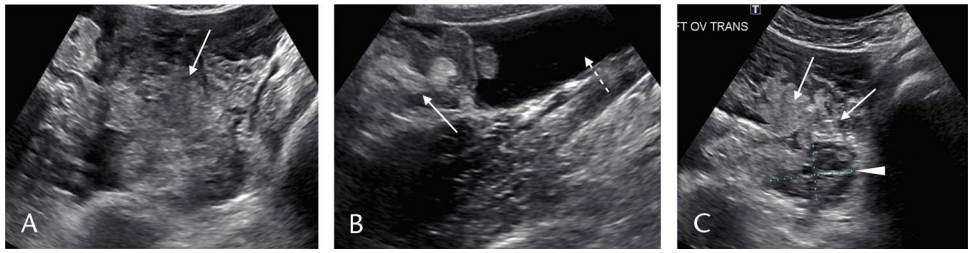

FIGURE 5. Acute ruptured hemorrhagic ovarian cyst with large clot formation and hemoperitoneum in a 16-year-old female patient. Transabdominal US images of the right adnexa in the transverse (A) and sagittal (B) planes show a complex hemorrhagic cyst with a large clot (white arrows) and adjacent free fluid in the right lower quadrant (white dotted arrow), suggestive of hemoperitoneum. C, Transverse TAS shows the normal left ovary (white arrowhead) with adjacent heterogeneous clot (white arrows).

with enhancing walls and complex fluid, as well as associated pelvic fat stranding, thickening of the uterosacral ligaments, and possible reactive small bowel ileus (Figs. 7 and 8).

Tubo-ovarian Abscess

If pyosalpinx is not adequately treated, inflammatory exudate, pus, blood, and debris continue to accumulate and may progress to form a tubo-ovarian abscess (TOA). Sonographic features of TOA include a complex adnexal mass with solid and cystic components characterized by internal septa, irregular mural thickening, a fluid-debris level, or inflammatory changes with surrounding echogenic fat. The ipsilateral fallopian tube and ovary may not be distinguishable entities, but diagnostic certainty increases if concomitant pyosalpinx is identified. Computed tomography and MRI may additionally show enhancing walls, septations, and thickening of the adjacent uterine ligaments or peritoneum.

Compared with other pelvic abscesses, TOAs are located near the adnexa with thinner walls, rare internal gas bubbles with debris, and possible anterior displacement of the broad ligament. Radiologic findings overlap with those for other pelvic cystic masses and should be correlated clinically with findings of fever, leukocytosis, and cervical motion tenderness. Tubo-ovarian abscesses may be managed conservatively with antibiotics, with percutaneous drainage or surgical resection reserved for persistent or life-threatening infection[16] (Fig. 9).

In children, pelvic abscesses may also occur because of inflammatory bowel disease (IBD) or infections of the appendix, colon, rectum, or (rarely) bladder. On US, these abscesses appear as hypoechoic fluid collections with thicker walls and more common internal gas bubbles and debris. These are often managed with percutaneous image-guided drainage, particularly in IBD (Figs. 19 and 24).

Hematosalpinx

Hematosalpinx occurs when an obstructed fallopian tube becomes distended with blood, often caused by cloacal abnormalities in pediatrics. Other typical etiologies include tubal

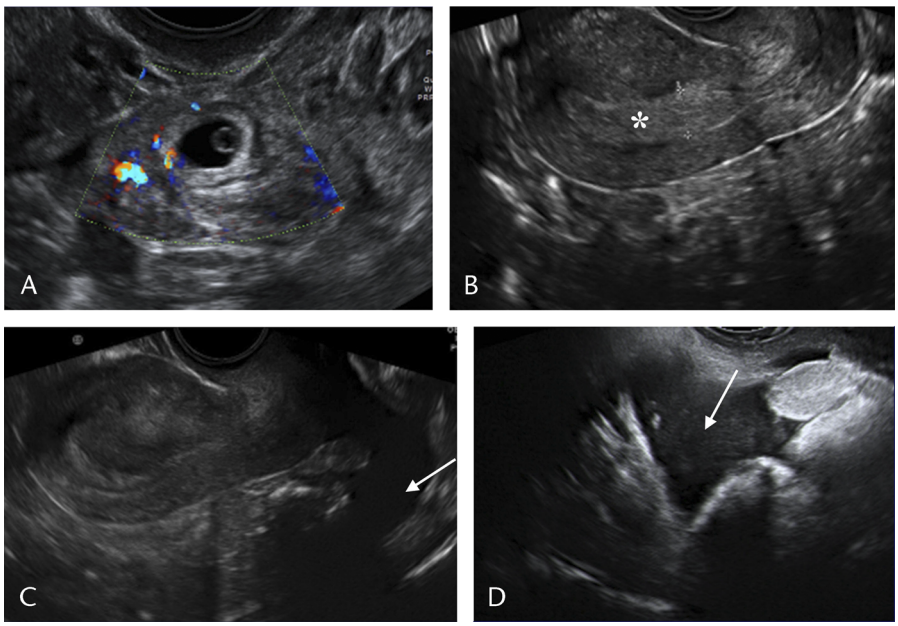

FIGURE 6. Ruptured tubal ectopic pregnancy in an 18-year-old female patient. Transvaginal transverse US images demonstrate a tubal ectopic pregnancy with peripheral vascularity on color Doppler (A) and decidual reaction (*) in the uterus (B). Free fluid with internal echoes (white arrows) represents hemoperitoneum in the cul-de-sac (C) and lower quadrant (D), consistent with rupture.

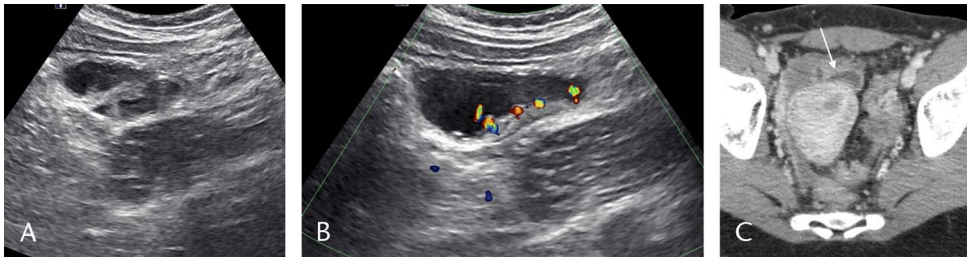

FIGURE 7. Right pyosalpinx in a 17-year-old female patient presenting with pelvic pain and vaginal discharge. Transabdominal transverse US images (A, B) show a distended, serpiginous, tubular structure in the right lower quadrant with thickened walls, complex fluid, and layering echogenic debris with internal vascularity on color Doppler. Axial CT (C) in the same patient shows an enhancing, thick-walled, dilated fallopian tube (white arrow) with adjacent high-attenuation free pelvic fluid.

endometriosis, ectopic pregnancy, PID, adnexal torsion, malignancy, or trauma.

Ultrasound demonstrates a tubular serpiginous structure with homogeneous internal echoes, similar to the sonographic appearance of pyosalpinx but without mural hyperemia. On CT, a tubular adnexal structure distinct from the ovary may be identified containing high-attenuation fluid. Hematosalpinx can be difficult to distinguish from pyosalpinx, and MRI is the modality of choice for differentiating blood products from pus. Fat-saturated T1- and T2-weighted MRI will show hyperintense distended fallopian tubes. T2 shading, seen in endometriomas, is not usually present[17] (Fig. 10).

Hematometrocolpos

Hematometra and hematocolpos refer to distention of the uterus and/or vagina, respectively, with blood products. This usually results from obstructive müllerian abnormalities, including imperforate hymen, transverse vaginal septum, vaginal atresia, or a rudimentary uterine horn. Imperforate hymen is the most common female congenital reproductive anomaly and leads to hematometrocolpos at the onset of menses if not corrected earlier. On US, the uterus and/or vagina are markedly distended with hypoechoic fluid with internal echoes proximal to the site of obstruction. Blood products of varying ages may be identified as echogenic blood clots or fluid-fluid levels (Fig. 11).

Transperineal sonography, also called translabial sonography, can be used in conjunction with TAS for more detailed evaluation of lower urogenital tract and anorectal anatomy, using high-frequency linear array transducers (≥8 MHz). Transperineal sonography is well established in diagnosing patients with vaginal atresia, although imperforate hymen and transverse vaginal septum may also be diagnosed. Although MRI is often the preferred modality for evaluating müllerian abnormalities, transperineal sonography should be considered as a viable alternative, particularly in the initial US evaluation.[18]

URINARY TRACT ETIOLOGIES

Obstructing Calculi

Obstructing calculi at the ureterovesical junction (UVJ) can cause severe pelvic pain. Extracorporeal shock-wave lithotripsy is sometimes used to treat renal calculi, and UVJ calculi may be present after lithotripsy. Ureterovesical junction obstruction can lead to further complications of pyonephrosis, pyelonephritis, urinoma, calyceal rupture, or renal abscess formation.

On US, a calculus appears as an echogenic focus with posterior acoustic shadowing within the UVJ, possibly with adjacent focal bladder wall edema. Twinkle artifact may be present on color Doppler, as a discrete focus of alternating colors due to intrinsic noise within the US Doppler circuitry, although specificity increases when associated with a hyperechoic focus.[19] High-grade UVJ obstruction can lead to an absent ipsilateral ureteral jet on Doppler and upstream hydronephrosis. Ultrasound is less sensitive for the detection of urinary tract calculi, and additional evaluation with low-dose non-contrast CT may be needed for diagnosis or identification of further complications (Fig. 12).

Cystitis

Urinary tract infections are another common source of pelvic pain in pediatric patients. After a clinical diagnosis of

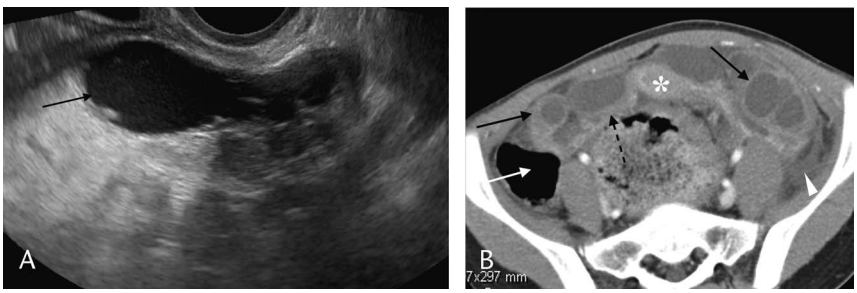

FIGURE 8. Bilateral pyosalpinx related to PID in a 17-year-old female patient. A, Transvaginal sagittal US image shows a dilated left adnexal tubular structure (black arrow) containing complex fluid and debris, compatible with pyosalpinx. B, Postcontrast axial CT shows a uterus (*) with dilated bilateral fallopian tubes with thick enhancing walls (black arrows) and ill-defined margins. A thickened broad ligament (black dotted arrow), fat stranding (white arrowhead), and focal small bowel ileus (white arrow) are seen.

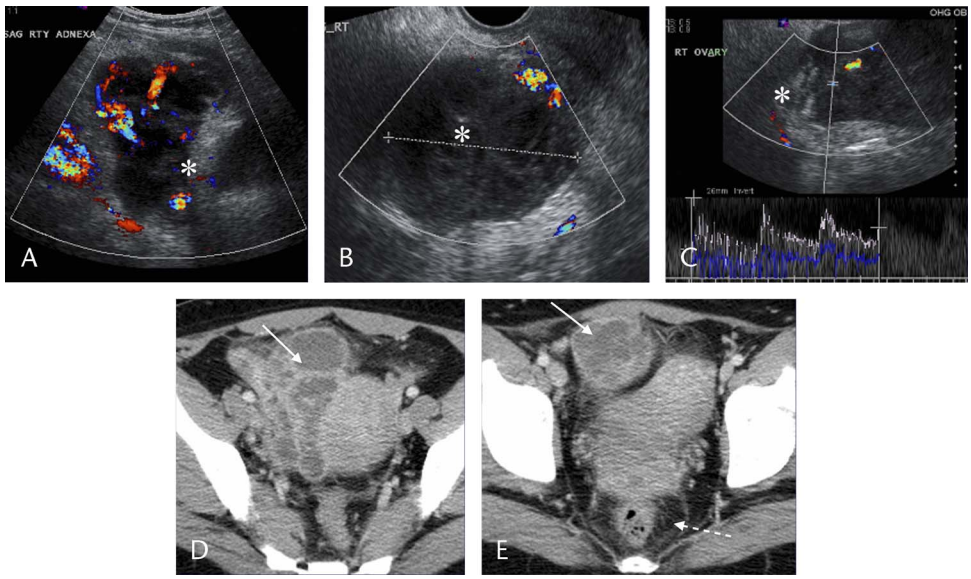

FIGURE 9. Tubo-ovarian abscess in a 15-year-old female patient. Transabdominal (A) and transvaginal (B, C) sagittal US images with color and spectral Doppler demonstrate a complex right adnexal lesion (asterisk) replacing the right ovary with hyperemia and decreased resistive index. Contrast-enhanced axial CT (D, E) reveals a peripherally enhancing complex cystic mass (white arrows) with an adjacent tubular component and presacral fat stranding (white dotted arrow), representing a TOA with associated pyosalpinx.

cystitis with laboratory evaluation, US may be used to screen for gross structural abnormalities of the kidneys, ureters, and bladder.

On US, diffuse bladder wall thickening, internal debris, and decreased bladder capacity confirm the clinical diagnosis of cystitis. Computed tomography or MRI can be used to evaluate further for anatomic causes of recurrent cystitis. Voiding cystourethrography or nuclear scintigraphy may later be performed to rule out vesicoureteral reflux and ascending infection if hydronephrosis, renal scarring, or high-grade obstruction is identified on US (Fig. 13).

In some instances, bladder wall thickening may be more focal and masslike on US. Urothelial cancers are uncommon in children, and nonneoplastic causes of polypoid growth should be considered, including infection, radiation, and bladder outlet obstruction. Cystitis cystica is a benign proliferative lesion with a typical US appearance of focal wall thickening with submucosal cyst formation, occurring in patients with chronic urothelial inflammation such as from recurrent infections or urinary tract calculi (Fig. 14).

GASTROINTESTINAL ETIOLOGIES

In patients with pelvic pain, the presentation and clinical evaluation may lead clinicians to initially focus on genitourinary pathologies. Imaging studies may be the first indicator of a GI etiology, suggesting a different algorithm for workup.

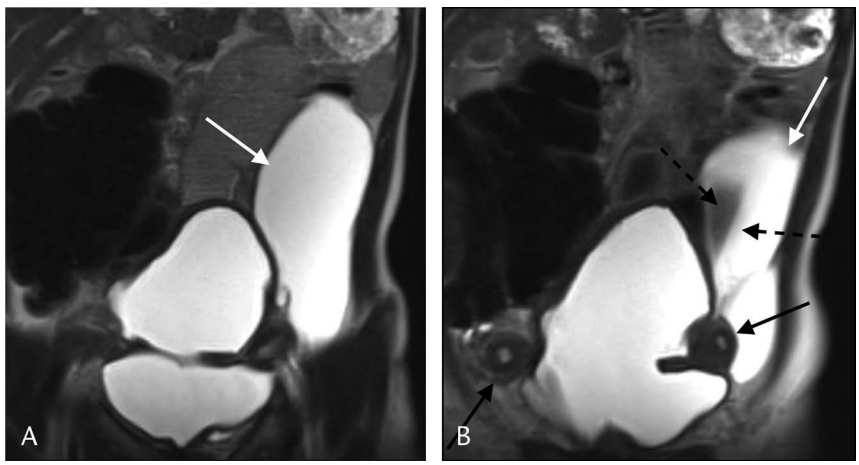

FIGURE 10. Bicornuate uterus with left hematosalpinx in a 13-year-old patient with cloacal and müllerian anomalies. Coronal T2-weighted MRI (A, B) shows a bicornuate uterus with 2 uterine horns (black arrows) and a T2-hyperintense dilated left fallopian tube (white arrows) containing blood products of different ages (black dotted arrows).

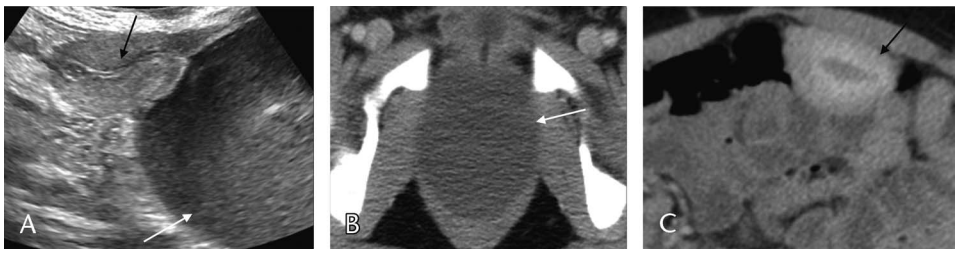

FIGURE 11. Hematocolpos in an 11-year-old female patient presenting with severe pelvic pain. Transabdominal US in the sagittal plane (A) shows marked dilatation of the vagina (white arrows) with low-level internal echoes, with a nondilated adjacent cervix and uterus (black arrows). Contrast-enhanced axial CT images (B, C) confirm the diagnosis of hematocolpos in this patient with imperforate hymen.

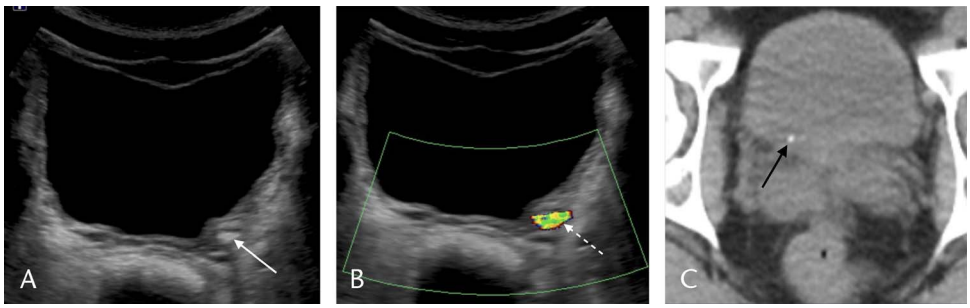

FIGURE 12. Ureterovesical junction calculus in a 7-year-old boy causing severe pelvic pain. Transabdominal transverse US images of the urinary bladder (A) with color Doppler (B) demonstrate a small echogenic calculus (white arrow) at the left UVJ, which shows twinkle artifact (white dotted arrow). C, In a different patient, low-dose noncontrast axial CT shows a focal calcific density within the right posterior bladder wall (black arrow) representing a UVJ calculus.

A brief review of relevant GI pathologies and their imaging features follow.

Bowel Obstruction

Bowel obstruction is characterized by GI tract dilatation proximal to the site of obstruction with the accumulation of air and/or fluid within the bowel lumen. In patients presenting with pelvic pain, distal small bowel and colonic obstruction are possible causes. In neonates, bowel obstruction is generally caused by congenital etiologies, such as bowel atresia or Hirschsprung disease. Older children present with lower GI tract obstruction due to more variable causes, including adhesions, appendicitis, intussusception, IBD, Meckel diverticulum, sigmoid volvulus, inguinal hernia, or foreign body ingestion. Radiography is the initial imaging test of choice, followed by further evaluation with fluoroscopy, CT, MRI, or US for identifying location, etiology, and complications.

Ultrasound may not be as helpful in most cases of mechanical bowel obstruction, as bowel gas often prevents a diagnostic-quality examination. In patients without significant

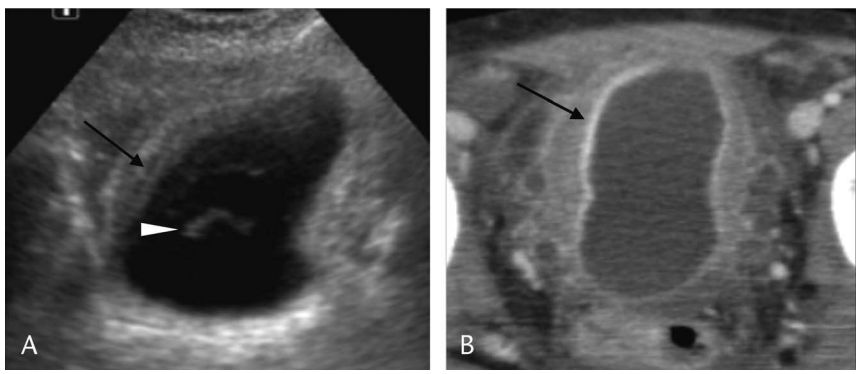

FIGURE 13. Uncomplicated cystitis in a 5-year-old boy. Transabdominal transverse gray-scale US (A) shows focal bladder wall thickening (black arrow) with internal debris (white arrowhead). Postcontrast axial CT (B) shows wall thickening and enhancement of the urinary bladder (black arrow).

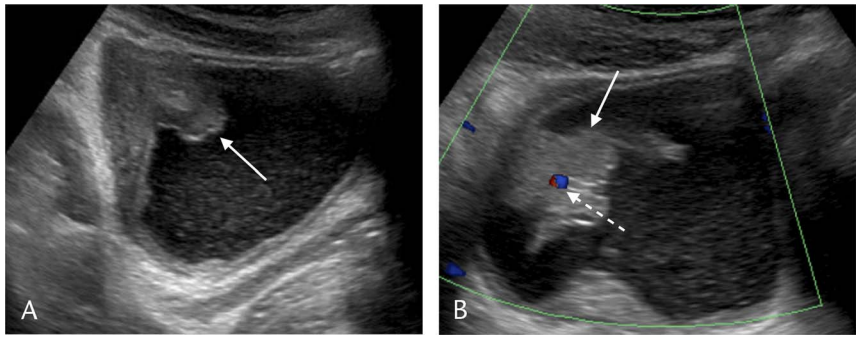

FIGURE 14. Cystitis cystica in a 3-year-old boy. Transabdominal sagittal US (A) exhibits focal wall thickening and internal debris within the urinary bladder, with a polypoid growth at the fundus (white arrows) that shows internal vascularity (white dotted arrow) on transverse color Doppler (B). Biopsy revealed cystitis cystica.

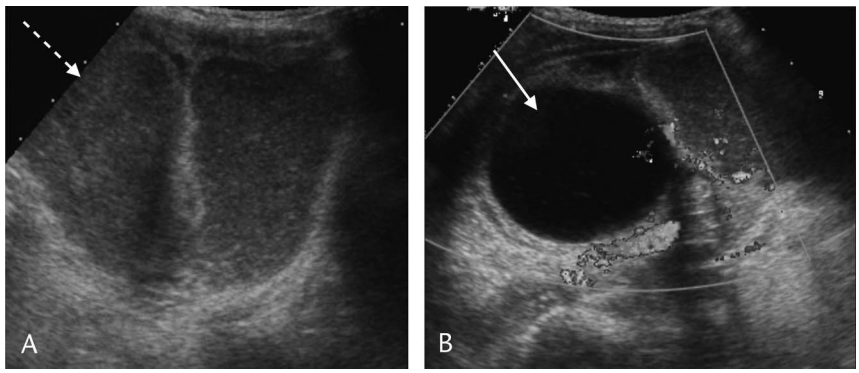

FIGURE 15. Bowel obstruction in a 5-year-old girl secondary to enteric duplication cyst. Transabdominal sagittal US image (A) demonstrates a small bowel obstruction with a dilated, fluid-filled, aperistaltic loop of bowel (white dotted arrow). In the right lower quadrant, sagittal color Doppler image (B) shows a hypoechoic cystic structure with gut signature and no internal vascularity, suggestive of enteric duplication cyst (white arrow) as the cause of obstruction.

gaseous distention, however, US can be used to assess bowel caliber and contents, site and possible etiology of obstruction, and location of bowel loops within the abdomen or within an external hernia. Evaluation of peristaltic activity may reveal early hyperperistalsis in obstruction or later diminished peristalsis after bowel exhaustion and overdistention. Ultrasound evaluation of bowel obstruction may additionally be helpful in diagnosing etiologies with typical sonographic findings, such as in intussusception, appendicitis, inguinal hernia, and so on[1] (Figs. 15 and 16).

Appendicitis

Acute appendicitis is the most common cause of acute abdomen requiring urgent or emergent surgery in children. Prompt

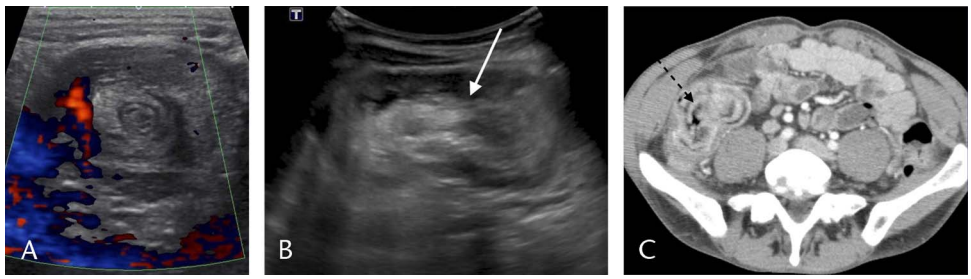

FIGURE 16. Three different patients with intussusception. A, A 3-year-old boy: transabdominal transverse US in the right lower abdomen shows an ileocolic intussusception with the typical "target sign" showing alternating concentric layers of bowel wall. B, In another patient, transabdominal sagittal US shows an ileocolic intussusception in longitudinal axis with invagination of ileum (white arrow) into a loop of ascending colon. C, Axial CT in a different patient with cystic fibrosis shows colocolic intussusception seen in cross section (black dotted arrow), similar to the sonographic target sign with alternating layers of telescoped bowel, fat, and bowel.

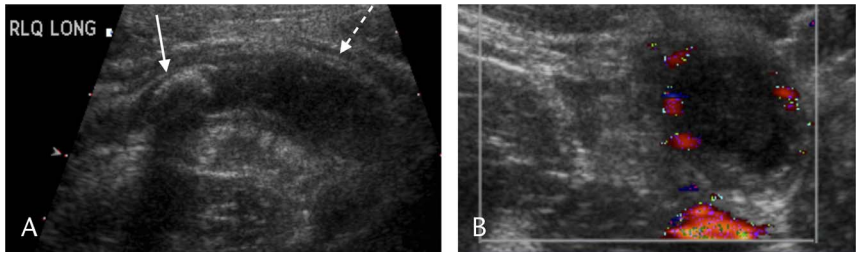

FIGURE 17. Acute uncomplicated appendicitis in a 6-year-old girl. Gray-scale sagittal US image (A) and transverse color Doppler (B) scan obtained with a high-frequency linear probe show a dilated appendix (white dotted arrow) with a proximal appendicolith (white arrow) and surrounding echogenic fat. The appendiceal wall is intact and hyperemic with no adjacent free fluid, lymphadenopathy, or abscess.

diagnosis is essential to preventing complications including perforation, sepsis, bowel obstruction, and appendiceal abscess.

Graded-compression sonography was first introduced in 1986 as a technique for diagnosing appendicitis and is still the preferred initial diagnostic modality in pediatric patients.[20] In this technique, a linear probe is placed at the site of maximal tenderness, and gradual compression is applied to displace overlying bowel and bowel gas; this may be used in conjunction with posterior manual compression for further displacement of bowel. When these techniques are unsuccessful in identifying the appendix, scanning a patient in the left oblique lateral decubitus position allows medial displacement of the cecum and terminal ileum and can help locate a retrocecal appendix.

Ultrasound findings of appendicitis include an immobile, noncompressible, and distended blind-ending tube with wall thickening (>2 mm) arising from the base of the cecum with focal probe tenderness. Secondary signs of inflammation include adjacent echogenic fat, hyperemia, and enlarged lymph nodes. Appendiceal diameter greater than 6 or 7 mm is sometimes used as a threshold for dilatation; however, size is less important in the absence of inflammation or other supportive features. The presence of an appendicolith is important to note for clinical management, regardless of appendiceal appearance.[1]

FIGURE 18. Acute appendicitis within an Amyand hernia in a 17-year-old male patient. Axial (A), coronal (B, C), and sagittal (D) CT images demonstrate a herniated, thick-walled appendix in the right inguinal canal (white arrows) with adjacent inflammatory changes (white dotted arrows).

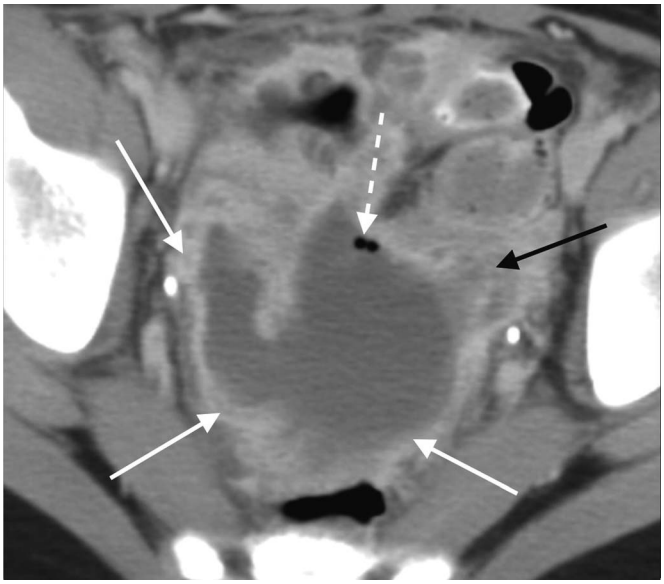

FIGURE 19. Appendicular abscess in an 11-year-old male patient postappendectomy. Axial CT scan shows a large homogeneous low-attenuation fluid collection with thick irregular enhancing walls (white arrows) and locules of air (white dotted arrow) in the nondependent portion of the pouch of Douglas with adjacent inflammatory changes (black arrow). The abscess was drained using a percutaneous transgluteal approach.

Ultrasound is considered negative for appendicitis when a normal, compressible appendix is visualized in full extent; US is considered equivocal or nondiagnostic when the appendix is not seen or not evaluated in full extent. In cases of equivocal US, persistent clinical concern, or patients at high clinical risk, stepwise evaluation with CT or MRI may follow[21] (Figs. 17–19).

Meckel Diverticulitis

Meckel diverticulum is a remnant of the omphalomesenteric duct, more common in males than in females. When inflamed, typical presentation is before age 10 years with abdominal or pelvic pain and/or GI bleeding. It is the most common cause of GI bleed in pediatric patients, and it remains the most common GI tract malformation, occurring in 2% to 3% of the population.[22] Meckel diverticulum is a true diverticulum, usually occurring along the antimesenteric border of the distal ileum; it may contain heterotopic gastric or pancreatic mucosa. Complications include diverticulitis, hemorrhage from peptic ulceration, bowel obstruction, intussusception, volvulus, torsion, herniation, and neoplasia.

Ultrasound shows a blind-ending tubular structure with gut signature arising from the distal ileum. If inflamed as in Meckel diverticulitis, additional US findings may include noncompressibility, adjacent echogenic fat, and hyperemia. If the distal ileum is not properly identified at the base of the diverticulum, findings can mimic appendicitis.

Heterotopic gastric mucosa can be seen in 20% of Meckel diverticula.[23] In patients who present with GI bleed, technetium 99m pertechnetate scintigraphy (Meckel scan) is the initial study

FIGURE 20. Meckel diverticulitis: 3 different patients and 3 different modalities. A, A 5-year-old boy: gray-scale transverse US of the right lower quadrant demonstrates a dilated tubular structure with gut signature (white dotted arrow), containing complex fluid with internal echoes. Differential diagnoses include duplication cyst. B, A 7-year-old girl: axial CT scan displays an enhancing tubular structure (black arrow) in the right lower quadrant with focal fat stranding (black arrow). Surgery revealed an inflamed Meckel diverticulum and normal appendix. C, A 2-year-old boy: technetium 99m pertechnetate scan in a patient with lower GI bleeding exhibits focal radiotracer activity in the right lower quadrant (white arrows).

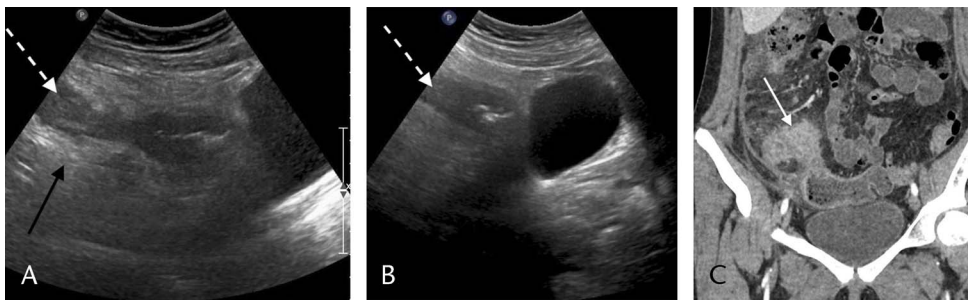

FIGURE 21. Pelvic pain and active Crohn disease in a 17-year-old female patient. Gray-scale sagittal US images (A, B) of the right pelvis show a dilated fluid-filled loop of small bowel (white dotted arrows) with bowel wall thickening and creeping echogenic fat (black arrow). Same-day contrast-enhanced axial CT scan (C) demonstrates inflammation of the terminal ileum (white arrow) with marked mesenteric fat stranding, concerning for active IBD.

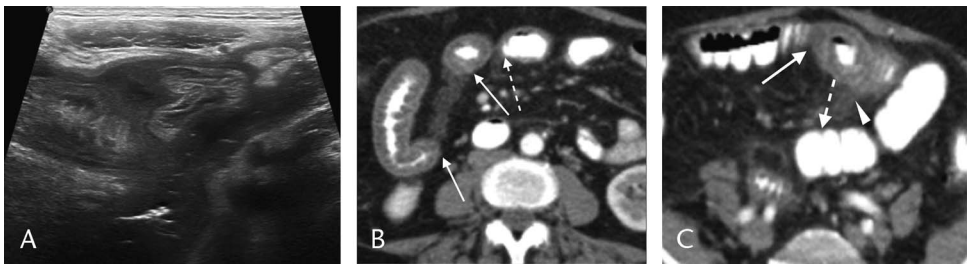

FIGURE 22. New diagnosis of Crohn disease in a 17-year-old female patient. A, Transabdominal transverse US image shows prominent wall thickening in multiple loops of small bowel. B and C, Postcontrast axial CT scan demonstrates multiple areas of inflammatory strictures (white arrows) with skip areas (white dotted arrow) and adjacent fat stranding (white arrowhead).

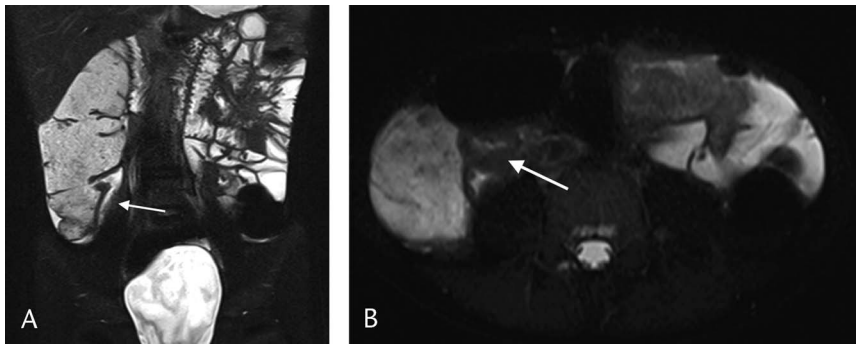

FIGURE 23. Terminal ileitis in a 10-year-old girl with Crohn disease. Coronal (A) and axial (B) T2-weighted images from magnetic resonance enterography demonstrate wall thickening of the terminal ileum (white arrows).

of choice when Meckel diverticulitis is clinically suspected. Patients presenting with abdominal or pelvic pain will likely undergo US and/or CT first, however, and radiologists should consider recommending a confirmatory Meckel scan if suggestive imaging features are present. Positive Meckel scans will show focal pertechnetate uptake and secretion by ectopic gastric mucosa in the expected location within the right lower abdomen (Fig. 20).

Inflammatory Bowel Disease

Crohn disease and ulcerative colitis are commonly diagnosed in adolescence and young adulthood, with incidence in younger pediatric patients on the rise.

As US is often the initial imaging study performed in any pediatric patient with acute abdominal or pelvic complaints, a new diagnosis of IBD may be suggested first by US. Findings include concentric bowel wall thickening, creeping fat along bowel margins, hyperemia, lymphadenopathy, and complications such as inflammatory masses, strictures, and perforation.[1] In addition, US has increasingly been gaining favor with GI specialists as a surveillance modality in the colon, with bowel wall thickening (>3 mm) correlating with active inflammation with high sensitivity and specificity when using colonoscopy as the reference standard[24] (Figs. 21 and 22).

Ultrasound surveillance is not yet widely used, however. Other cross-sectional modalities are helpful in further characterizing intraluminal and extraluminal disease extent and identifying complications such as phlegmon, abscess, sinus tract, and fistula formation.

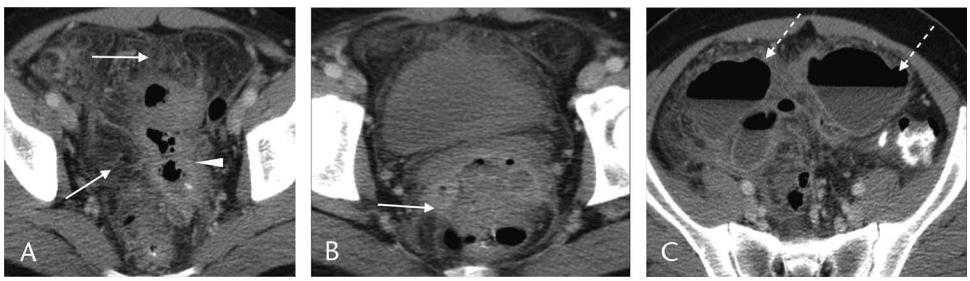

FIGURE 24. Pelvic abscesses in a patient with penetrating Crohn disease. Axial CT demonstrates (A, B) rectosigmoid wall thickening (white arrowhead) and pericolonic fat stranding (white arrows) with (C) multiple pelvic abscesses containing air and fluid (white dotted arrows). The abscesses were drained via CT-guided percutaneous catheter placement with subsequent resolution.

Magnetic resonance enterography has replaced CT enterography as the modality of choice in serial monitoring because of lack of ionizing radiation, improved imaging resolution, evaluation of peristalsis, and frequency of imaging required in children with IBD. Expected findings include segmental bowel wall thickening, mural stratification, mucosal hyperenhancement, skip lesions, luminal narrowing or strictures, and fistulas. Diffusion-weighted imaging can help identify active small bowel inflammation, which is more common to Crohn disease[25] (Figs. 23 and 24).

CONCLUSION

Nontraumatic pelvic pain in pediatric patients can result from a range of reproductive, urinary, and GI tract pathologies. Transabdominal sonography is often the initial imaging study performed in evaluating pelvic pain, sometimes used in conjunction with transvaginal, transperineal, or retroperitoneal techniques. Prompt evaluation and diagnosis of pelvic pathology are important on the part of the radiologist to expedite emergent care and prevent morbidity and mortality. The examples presented in our pictorial review will help radiologists be aware of common appearances of pelvic pathologies encountered in the pediatric population.

ACKNOWLEDGMENT

The authors thank Dr Ameya Baxi for introducing the concept of nontraumatic pediatric pelvic emergencies as a review topic.

REFERENCES

1. Rosenberg HK. Pediatric pelvic sonography. In: Rumack C, Levine D, eds. *Diagnostic Ultrasound*. 3rd ed. Elsevier; 2003:1977–2033.
2. Gilligan LA, Trout AT, Schuster JG, et al. Normative values for ultrasound measurements of the female pelvic organs throughout childhood and adolescence. *Pediatr Radiol*. 2019;49:1042–1050.
3. Langer JE, Oliver ER, Lev-Toaff AS, et al. Imaging of the female pelvis through the life cycle. *Radiographics*. 2012;32(6):1575–1597.
4. Chen M, Chen CD, Yang YS, et al. Torsion of the previously normal uterine adnexa. Evaluation of the correlation between the pathological changes and the clinical characteristics. *Acta Obstet Gynecol Scand*. 2001;80(1):58–61.
5. Oltmann SC, Fischer A, Barber R, et al. Cannot exclude torsion—a 15-year review. *J Pediatr Surg*. 2009;44(6):1212–1216.
6. Sisler CL, Siegel MJ. Ovarian teratomas: a comparison of the sonographic appearance in prepubertal and postpubertal girls. *AJR Am J Roentgenol*. 1990;154(1):139–141.
7. Servaes S, Zurakowski D, Laufer MR, et al. Sonographic findings of ovarian torsion in children. *Pediatr Radiol*. 2007;37:446–451.
8. Stark JE, Siegel MJ. Ovarian torsion in prepubertal and pubertal girls: sonographic findings. *AJR Am J Roentgenol*. 1994;163(6):1479–1482.
9. Patel MD, Feldstein VA, Filly RA. The likelihood ratio of sonographic findings for the diagnosis of hemorrhagic ovarian cysts. *J Ultrasound Med*. 2005;24(5):607–614.
10. Potter AW, Chandrasekhar CA. US and CT evaluation of acute pelvic pain of gynecologic origin in nonpregnant premenopausal patients. *Radiographics*. 2008;28(6):1645–1659.
11. Bouyer J, Coste J, Fernandez H, et al. Sites of ectopic pregnancy: a 10 year population-based study of 1800 cases. *Hum Reprod*. 2002;17:3224–3230.
12. Garel L, Dubois J, Grignon A, et al. US of the pediatric female pelvis: a clinical perspective. *Radiographics*. 2001;21(6):1393–1407.
13. Levine D. Ectopic pregnancy. *Radiology*. 2007;245:385–397.
14. Attar E. Endocrinology of ectopic pregnancy. *Obstet Gynecol Clin North Am*. 2004;31(4):779–794.
15. Ratani RS, Cohen HL, Fiore E. Pediatric gynecologic ultrasound. *Ultrasound Q*. 2004;20(3):127–139.
16. Lareau SM, Beigi RH. Pelvic inflammatory disease and tubo-ovarian abscess. *Infect Dis Clin North Am*. 2008;22(4):693–708.
17. Rezvani M, Shaaban AM. Fallopian tube disease in the nonpregnant patient. *Radiographics*. 2011;31(2):527–548.
18. Son JK, Taylor GA. Transperineal ultrasonography. *Pediatr Radiol*. 2014;44 (2):193–201.
19. Dillman JR, Kappil M, Weadock WJ, et al. Sonographic twinkling artifact for renal calculus detection: correlation with CT. *Radiology*. 2011;259(3):911–916.
20. Puylaert JB. Acute appendicitis: US evaluation using graded compression. *Radiology*. 1986;158(2):355–360.
21. Krishnamoorthi R, Ramarajan N, Wang NE, et al. Effectiveness of a staged US and CT protocol for the diagnosis of pediatric appendicitis: reducing radiation exposure in the age of ALARA. *Radiology*. 2011;259(1):231–239.
22. Levy AD, Hobbs CM. From the archives of the AFIP. Meckel diverticulum: radiologic features with pathologic correlation. *Radiographics*. 2004;24(2): 565–587.
23. Cserni G. Gastric pathology in Meckel's diverticulum. Review of cases resected between 1965 and 1995. *Am J Clin Pathol*. 1996;106:782–785.
24. Sagami S, Kobayashi T, Miyatani Y, et al. Accuracy of ultrasound for evaluation of colorectal segments in patients with inflammatory bowel diseases: a systematic review and meta-analysis. *Clin Gastroenterol Hepatol*. 2021;19(5):908–921.e6.
25. Towbin AJ, Sullivan J, Denson LA, et al. CT and MR enterography in children and adolescents with inflammatory bowel disease. *Radiographics*. 2013;33:1843–1860.